ISIJ International, Vol. 61 (2021), No. 8, pp. 2299–2304
https://doi.org/10.2355/isijinternational.ISIJINT-2020-780

Evaluation of Multiaxial Low Cycle Creep-fatigue Life for Mod.9Cr-1Mo Steel under Non-proportional Loading

Yuta NAKAYAMA,[1)] Fumio OGAWA,[2)]* Noritake HIYOSHI,[3)] Ryuta HASHIDATE,[4)] Takashi WAKAI[4)] and Takamoto ITOH[5)]

1) Graduate School of Science & Engineering, Ritsumeikan University, 1-1-1, Noji-higashi, Kusatsu-shi, Shiga, 525-8577 Japan.
2) Fracture and Reliability Research Institute, Graduate school of Engineering, Tohoku University, 6-6-11 Aza-Aoba Aramaki, Aoba-ku, Sendai-shi, Miyagi, 980-8579 Japan.
3) Division of Engineering, Faculty of Engineering, University of Fukui, 3-9-1, Bunkyo, Fukui-shi, Fukui, 910-8507 Japan.
4) Japan Atomic Energy Agency, 4002 Narita-cho, O-arai, Ibaraki, 311-1393 Japan.
5) Department of Mechanical Engineering, College of Science and Engineering, Ritsumeikan University, 1-1-1, Noji-higashi, Kusatsu-shi, Shiga, 525-8577 Japan.

(*Received on January 7, 2021; accepted on May 11, 2021; J-STAGE Advance published date: June 19, 2021*)

This study discusses the creep-fatigue strength for Mod.9Cr-1Mo steel at a high temperature of 823 K under multiaxial loading. Low cycle fatigue tests in various strain waveforms were performed with a hollow cylindrical specimen. The tests were conducted under a proportional loading with a fixed axial strain and a non-proportional loading with a 90-degree phase difference between axial and shear strains. The tests at different strain rates and the creep-fatigue tests at different holding times were also conducted to discuss the effects of stress relaxation and strain holding on the failure life. In this study, two types of multiaxial creep-fatigue life evaluation methods were proposed: the first method is to calculate the strain range using Manson's universal slope method with considering a non-proportional loading factor and creep damage; the second method is to calculate the fatigue damage by considering the non-proportional loading factor using the linear damage law and to calculate the creep damage from the improved ductility exhaustion law. The accuracy of the evaluation methods is much better than that of the methods used in the evaluation of actual machines such as time fraction rule. The second method proposed by the authors showed the highest evaluation accuracy. The first evaluation equation is slightly less accurate than the second, but it is useful in that the evaluation procedure is easy.

KEY WORDS: creep-fatigue; life evaluation; multiaxial loading; non-proportional loading; Mod.9Cr-1Mo steel.

1. Introduction

Mod.9Cr-1Mo steel, known as typical high chromium ferritic heat-resistant steel, has a good balance between a high temperature strength and mechanical properties, and has been widely used in thermal power plants. Because the service conditions in such plants are complex due to mechanical stress and thermal stress, structure materials undergo the non-proportional multiaxial loading state in which the direction of the principal stresses and principal strains changes with time. It is reported that the fatigue life under non-proportional multiaxial loading is significantly lower than that under proportional loading. High temperature structural equipment in thermal power plants also suffers creep-fatigue damage due to the combination of cyclic stresses associated with start-up and shutdown and creep damage during steady-state operation.[1–11)] Therefore, in order to design and assure the integrity of high temperature structural equipment under such severe conditions, it is essential to establish an appropriate non-proportional multiaxial creep fatigue life evaluation method.

The universal slope method,[12)] the linear damage law,[13)] time fraction rule,[14)] the strain range partitioning method[15)] and other representatives creep-fatigue life evaluation methods have been proposed, and their validity and evaluation accuracy have been studied. However, there are little experimental data on non-proportional multiaxial loading at high temperatures and the applicability of these evaluation methods to the non-proportional multiaxial creep-fatigue loading that frequently occur in actual industrial machines have not been studied.

In this study, two types of non-proportional multiaxial

* Corresponding author: E-mail: fumio.ogawa.d8@tohoku.ac.jp

creep-fatigue life evaluation methods are proposed. The first method is based on Manson's universal slope method with a strain range that takes into account the effects of non-proportional loading factor and creep damage. However, the parameters used to evaluate creep damage are focused on simplicity and do not fully take into account the effects of creep. To modify the fatigue life evaluation accuracy, the fatigue damage is calculated using the linear damage law, and the creep damage is calculated using the modified ductility exhaustion model[16] in the second evaluation method. The applicability of these two evaluation methods to Mod.9Cr-1Mo steel at 823 K is discussed based on the multiaxial creep-fatigue test results.

2. Experimental Procedure

2.1. Material and Specimen

The material used in this study is Mod.9Cr-1Mo steel which is high chromium ferritic steel standardized in ASTM A213-83. Its chemical composition is shown in **Table 1**. Heat treatment was performed for a plate of Mod.9Cr-1Mo steel. The normalizing condition was 1 050°C for 1.08 h, while the tempering condition was 780°C for 1.42 h. Stress relief treatment was performed at 740°C for 10.6 h. **Figure 1** shows the shape and dimensions of the hollow cylinder specimen with an outer diameter of 12 mm, an inner diameter of 9 mm and a parallel portion length of 8 mm. The inner and outer surfaces of the specimens are polished with emery paper up to 2 000 grit, and the outer surface of the specimens is buffed with alumina particles up to 1 μm in diameter before the tests.

2.2. Testing Machine

Two types of electro-hydraulic servo-type multiaxial fatigue test machines are used in this study: one is capable of applying an axial load to the specimen by computer control, and the other is capable of applying both axial load and torsional torque. Axial and shear strains are measured using an extensometer, which has two eddy current displacement sensors. A high frequency induction heating system was used to heat the specimen. The temperature at the gauge section was controlled to 823 K by attaching a thermocouple to 4 mm below to the gauge section.

Table 1. Chemical composition of the material tested (wt.%).

C	Si	Mn	P	S	Cr
0.096	0.280	0.440	0.007	0.002	8.480
Ni	Mo	V	Nb	Al	N
0.050	0.880	0.200	0.076	0.005	0.050

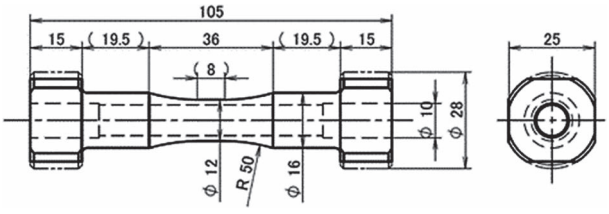

Fig. 1. Shape and dimensions of the specimen (mm).

Failure life is defined as the number of cycles when the axial stress amplitude decreased to 3/4 of that at the variation from steady state or specimen breakage observed.

2.3. Strain Waveforms

The loading mode are two types as shown in **Fig. 2**, they are the push-pull loading (PP) and the circle-shaped loading (CI). The PP test is the proportional strain loading test and the CI test is the non-proportional strain loading test in which axial strain (ε) and shear strain (γ) have 90° phase difference.

Figure 3 shows schematic image of strain waveforms for proportional and non-proportional loading. In PP tests, they were carried out with triangular waveforms with different strain rates, and with the waveforms holding strain on the tensile or compressive side. The strain rates in the tests without strain holding were 0.2%/s, 0.01%/s, and 0.002%/s. In this paper, they are denoted as PP-FF, PP-SS, and PP-SS*,

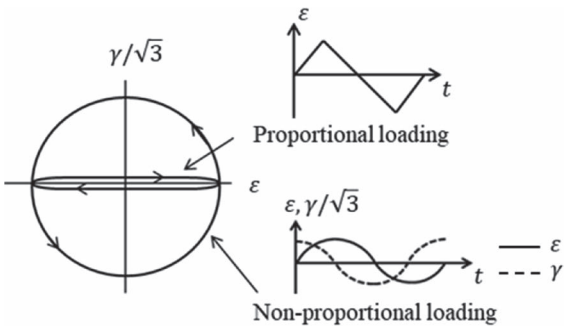

Fig. 2. Strain paths employed.

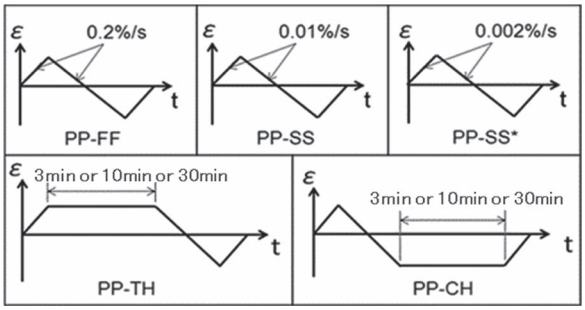

(a)

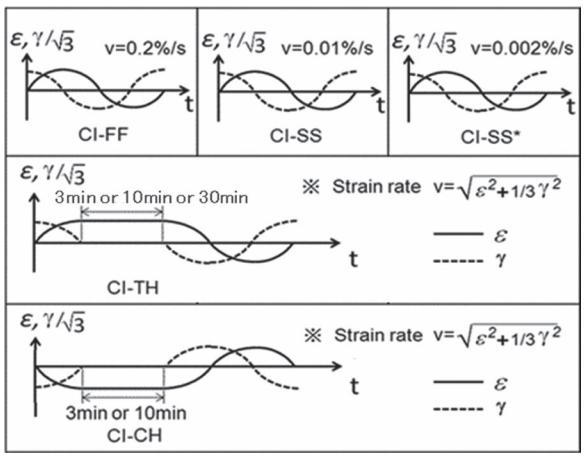

(b)

Fig. 3. Strain paths employed: (a) Proportional loading, (b) Non-proportional loading.

respectively. The strain holding times of the creep-fatigue test were 3, 10, and 30 minutes. In this paper, they are denoted as PP-TH (3 min), PP-TH (10 min), and PP-TH (30 min) for tensile holding tests and PP-CH (3 min), PP-CH (10 min), and PP-CH (30 min) for compression holding tests, respectively. The strain rate of tests with strain holding was 0.2%/s as well as that of PP-FF.

In CI tests, they were carried out with sine and cosine waveforms with different strain rates, and with the waveforms holding axial strain on the tensile or compressive side. The Mises equivalent strain rates in the tests without strain holding were 0.2%/s and 0.01%/s. In this paper, they are denoted as CI-FF and CI-SS, respectively. The axial strain holding times of the creep-fatigue test were 3, 10, and 30 minutes on the tensile side, and 3 and 10 minutes on the compressive side. In this paper, they are denoted as CI-TH (3 min), CI-TH (10 min), and CI-TH (30 min) for tensile holding tests and CI-CH (3 min) and CI-CH (10 min) for compression holding tests, respectively. The Mises equivalent strain rate of tests with axial strain holding were 0.2%/s. The Mises equivalent strain ranges in all the tests for both PP and CI tests were set to 0.7%.

3. Experimental Results and Discussion

3.1. Deformation Properties

Figure 4 shows stress amplitude variation with the cycle for PP and CI tests. The vertical axis shows the stress amplitude ratio ($\sigma_{eq}/\sigma_{eq\ max}$), which is the stress amplitude in one cycle divided by the maximum value in the test, and the horizontal axis shows the failure life ratio N/N_f.

Figures 4(a) and 4(b) show the effect of strain rate and holding time on the stress amplitude variation in PP tests, respectively. These figure show that the stress amplitude decreased with decreasing strain rate and increasing holding time. The stress amplitude decreased largely in PP-TH (10 min) than in PP-TH (3 min), but the stress decrease was similar to that in PP-TH (30 min). These results indicate that the creep damage in PP-TH (3 min) is smaller than those in other tensile strain holding tests.

Figures 4(c) and 4(d) show the effect of strain rate and holding time on stress amplitude variation in CI tests, respectively. These figures show that the decrease in stress amplitude with decreasing strain rate and the increasing holding time in the CI test was as large as that in the PP test. Thus, the effects of strain rate and tensile holding time on cyclic softening were not almost same but in similar tendency between PP and CI.

3.2. Creep-fatigue Life Results

Figure 5(a) shows the failure life in the PP test normalized by that in PP-FF test, and Fig. 5(b) shows the failure life in the CI test normalized by that in PP-FF test.

In Fig. 5(a), the failure life of PP-SS is slightly larger than that of PP-FF, and that of PP-SS* is about the same as that of PP-FF. In tensile holding tests (TH), PP-TH (3 min) had a larger life than PP-FF, and PP-TH (10 min) and PP-TH (30 min) had the same life as PP-FF. On the other hand, in compression-holding tests (CH), the life of PP-CH (3 min) was similar to that of PP-FF, but the failure life of PP-CH (10 min) and PP-CH (30 min) was significantly smaller than

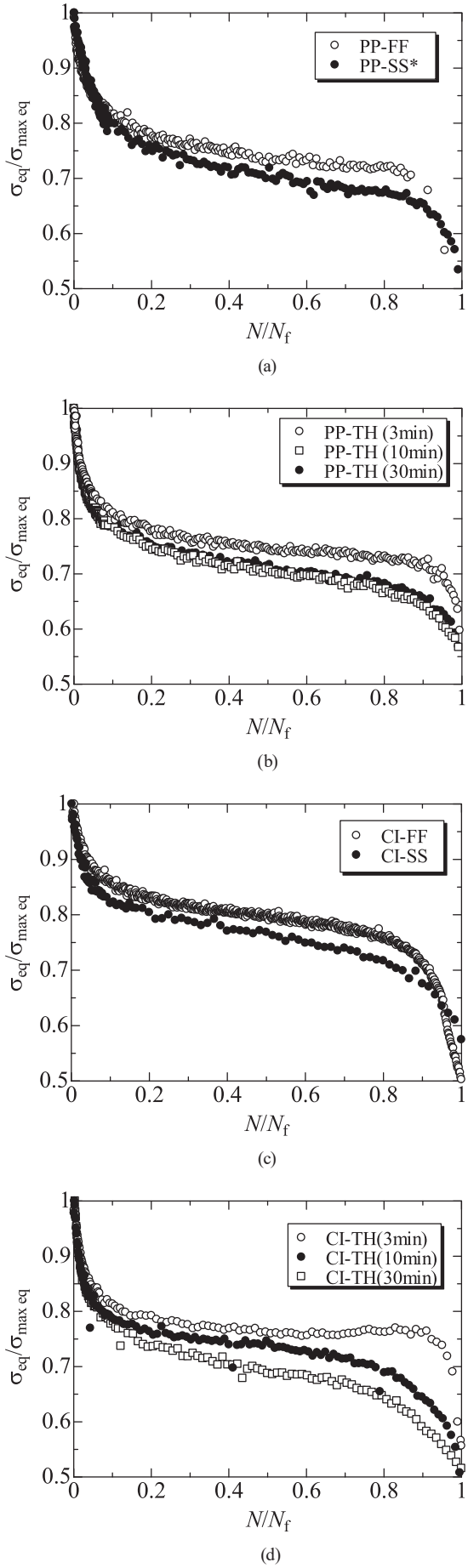

Fig. 4. Variation of stress with life ratio: (a) PP-FF and PP-SS*, (b) PP-TH (3 min), PP-TH (10 min) and PP-TH(30 min), (c) CI-FF and CI-SS, (d) CI-TH (3 min), CI-TH (10 min) and CI-TH(30 min).

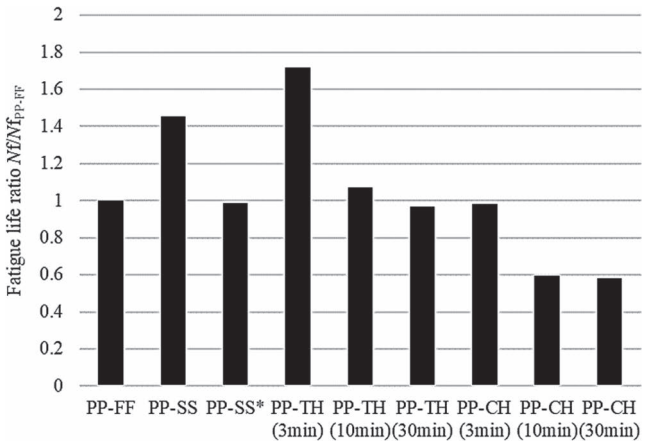

(a)

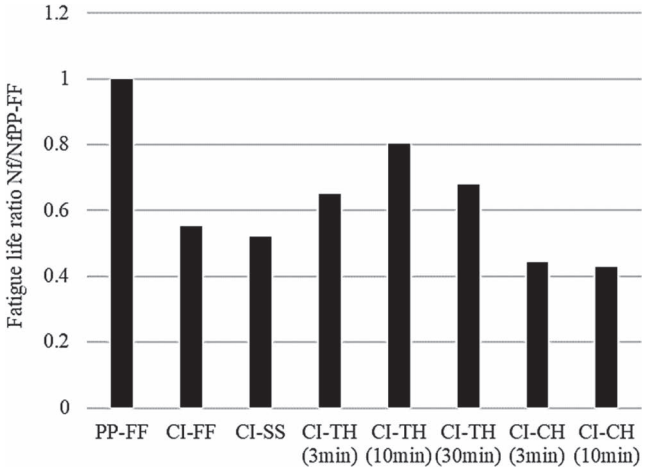

(b)

Fig. 5. Comparison of failure lives and variation of stress: (a) Push-Pull, (b) Circle.

that of PP-FF.

In Fig. 5(b), the failure life of CI-FF was about half of that of PP-FF, which is consistent with the results of previous studies.[17,18] This is due to the fact that in the CI test, the principal axes of both stress and strain are continuously rotated by one rotation during one cycle, which increases the number of active slip systems compared to the PP test, and consequently the number of cracks.[19–23] The life of CI-SS was comparable to that of CI-FF. In all tensile strain holding tests, the failure life of them was larger than that of CI-FF, and CI-TH (10 min) had the largest life. This can be attributed to the fact that the effect of non-proportional loading decreased with the increase in the effect of creep. In the non-proportional loading environment, the effect of creep deformation due to low strain rate and tensile holding mitigates the effect of principal axis direction change on failure life. This suggests an increase in the effect of creep and a decrease in the effect of non-proportionality, resulting in a larger failure life.[24] For the compression-holding tests, the failure life was lower than that of the CI-FF, as was the case for the PP test. However, it is presented that a decrease of failure life is not due to creep because this is reported to be due to mean stress and tensile strain developed during loading.[25]

3.3. Applicability of Present Fatigue Life Evaluation Method

The life prediction was performed by using the time fraction rule, which has been widely used in the evaluation of actual machines. The value calculated by the time fraction rule was used as the creep damage, and the number of failure cycles was estimated by the linear damage law. A comparison between the predicted life and the actual measured life is shown in **Fig. 6**. As shown in Fig. 6, the method predicts a shorter failure life than the actual failure life in many conditions, and the maximum error was about a factor of 5. Therefore, the method is specifically inappropriate for life prediction of non-proportional loading with strain holding.

4. Proposed Non-proportional Multiaxial Creep-fatigue Life Evaluation Method

4.1. NMCFLE Method

Manson's universal slope method, which is expressed as Eq. (1), is often used to estimate the cyclic failure life N_f.

$$\Delta\varepsilon = \frac{3.5\sigma_B}{E} N_f^{-0.12} + \varepsilon_f^{0.6} N_f^{-0.6} \quad \text{..... (1)}$$

where $\Delta\varepsilon$, σ_B, E, and ε_f is total strain range, the tensile strength, Young's modulus, fracture ductility, respectively. The Mises equivalent strain range ($\Delta\varepsilon_{eq}$) is used instead of $\Delta\varepsilon$ for multiaxial loading conditions such as the CI tests.

The non-proportional creep strain range ($\Delta\varepsilon_{NP}$) is used instead of $\Delta\varepsilon$ for non-proportional loading or creep conditions. $\Delta\varepsilon_{NP}$ which takes into account the effects of non-proportional loading and creep is expressed as follows.[17,26,27]

$$\Delta\varepsilon_{NP} = (1 + \alpha K_s f_{NP}) K_V \Delta\varepsilon_I \quad \text{..... (2)}$$

where $\Delta\varepsilon_I$ is the maximum principal strain range for non-proportional loading. α is a material constant that represents cyclic hardening or softening factor under non-proportional loading and is calculated as follows.

$$\alpha = S\frac{\sigma_B - \sigma_Y}{\sigma_B} \quad \text{..... (3)}$$

where σ_Y is the yield stress or 0.2% proof stress under uniaxial tensile test, and S is a material factor that takes into account differences in the crystal structure, with $S = 1$ for FCC. materials and $S = 2$ for BCC. materials.[17,26,27]

The f_{NP} called the non-proportional loading coefficient is a parameter that expresses the severity of the non-proportional loading of the strain path and calculated as follows.

$$f_{NP} = \frac{\pi}{2SI_{max} L_{path}} \int_C \left| \boldsymbol{e}_1 \times \boldsymbol{e}_R S_I(t) \right| ds, \quad L_{path} = \int_C ds \quad \text{... (4)}$$

where $S_I(t)$ is the maximum absolute value of principal stress and principal strain at time t and SI_{max} is the maximum value of $S_I(t)$ during one cycle of the load path. $\boldsymbol{e}_1$ and $\boldsymbol{e}_R$ are the unit vectors in the $S_I(t)$ the direction shown in **Fig. 7**. C is the integral path of the stress-strain path and "×" is the external product. L_{path} is the sum of the total path length. f_{NP} is the proportional loading factor and $0 < f_{NP} \leq 1$ for non-proportional loading.[17,26,27]

In addition, K_V and K_S are parameters that describe the creep effect on the effective strain rate and the degree of reduction in the effect of non-proportional loading due to

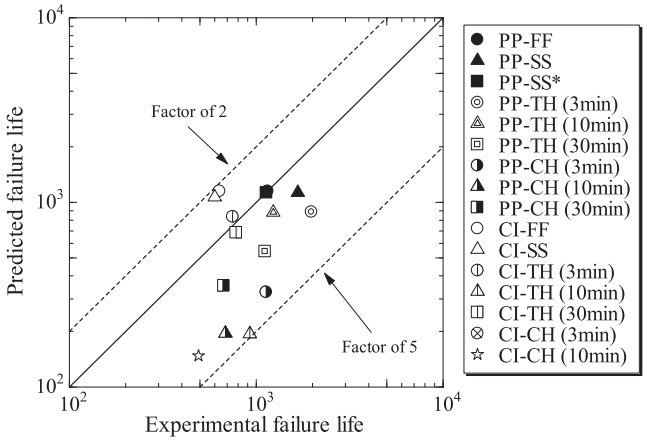

Fig. 6. Prediction by time fraction rule.

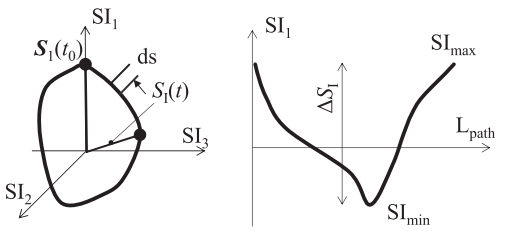

Fig. 7. Definitions of principal strain range and mean principal value.

creep relaxation.[28]

$$K_V = \left(\frac{v_1}{v_0}\right)^{(k-1)\beta} \quad \text{..... (5)}$$

$$K_S = \chi^{\left(\frac{v_1}{v_0}-1\right)} \quad \text{..... (6)}$$

where k, β and χ are material constants, derived from the experimental results of the PP and CI tests. v_0 is the testing frequency where creep damage can be neglected and v_1 is the test frequency of the test to be evaluated. This evaluation method is named "NMCFLE (Non-Proportional Multiaxial Creep-Fatigue Life Evaluation) Method".

4.2. Mod NMCFLE Method

Although the evaluation method proposed in the previous section is relatively easy to use for fatigue life estimation, especially for creep damage, the parameters used to evaluate creep damage are focused on simplicity and do not fully take into account the effects of creep. Therefore, a modified fatigue life evaluation method that takes into account the reduction in ductility and the relaxation curve during load holding are also proposed in this section.

A linear damage law is used to estimate the failure life (n). Components materials are considered to be damaged by the accumulation of fatigue damage (D_f) and creep damage (D_C), and its failure life is estimated as the point at which the accumulated value reaches to 1 in the law.

$$n = \frac{1}{D_f + D_c} \quad \text{..... (7)}$$

Multiaxial creep-fatigue life evaluation is attempted by defining D_f and D_c, respectively.

D_f is defined as Eq. (8) using the provisional failure life (N_f') at when creep damage does not occur.

$$D_f = \frac{1}{N_f'} \quad \text{..... (8)}$$

N_f' is derived using Eq. (1), and the $\Delta\varepsilon_{NP}$ in Eq. (1) is newly defined with the following parameters, taking into account the non-proportional load and the reduction of the non-proportional effect induced by creep.

$$\Delta\varepsilon'_{NP} = (1 + \alpha K_s f_{NP})\Delta\varepsilon_I \quad \text{..... (9)}$$

This parameter is derived from Eq. (2) by removing the variables for creep damage evaluation.

D_c is calculated using the modified ductility exhaustion law proposed by Takahashi *et al.*[16] based on the idea that the ductility reduction is due to creep damage.

$$D_c = \int_0^{t_H} \left|\frac{1}{\delta} - \frac{1}{\delta_0}\right| \dot{\varepsilon}_{in} dt \quad \text{..... (10)}$$

where t_H is the holding time of one cycle. In the relationship between rupture time and rupture ductility in creep tests, δ_0 is the rupture ductility at a sufficiently high strain rate where no creep damage is expected to occur, and δ is the rupture ductility at a long time after constant creep damage.

$\dot{\varepsilon}_{in}$ is the inelastic strain rate and requires a change in the inelastic strain rate during holding. To this end, we approximate the mid-life stress relaxation data for each test. From that approximation, the inelastic strain rate is defined as a function of time as follows.

$$\dot{\varepsilon}_{in} = \frac{Am\sigma_0 t^{m-1}}{E\exp(At^m)} \quad \text{..... (11)}$$

where σ_0 is the initial stress at the beginning of strain holding, A and m are the material constants calculated from the experimental stress relaxation curve fitting, E is the longitudinal modulus, and t is the elapsed time. Thus, creep damage is assessed by the degree of reduced ductility and creep relaxation. This evaluation method is called the "Mod NMCFLE (Modified Non-Proportional Multiaxial Creep-Fatigue Life Evaluation) Method" in this work.

4.3. Applicability of Proposed Fatigue Life Evaluation Method

A comparison of the predicted life and the measured life obtained by the NMCFLE Method is shown in **Fig. 8**. Almost all the tests were evaluated within a factor of 2, although only a few of them were evaluated within the range of a factor of 1.5. The figure also shows that the failure life of most of the tensile and holding tests tends to be evaluated on the conservative side. It is suggested that the creep damage was overestimated because the effect of creep on the tensile hold was small in this study.

A comparison of the predicted and measured life obtained by the Mod NMCFLE Method is shown in **Fig. 9**. It can be seen that almost all the tests were evaluated within a factor of 2 scatter band, and the number of failure lives evaluated within a factor of 1.5 increased compared to the life prediction results in Fig. 8. Furthermore, it can be seen from the same figure that all the tests with non-proportional loading are evaluated within a factor of 1.5. This result indicates that the proposed method in this work can predict the failure life

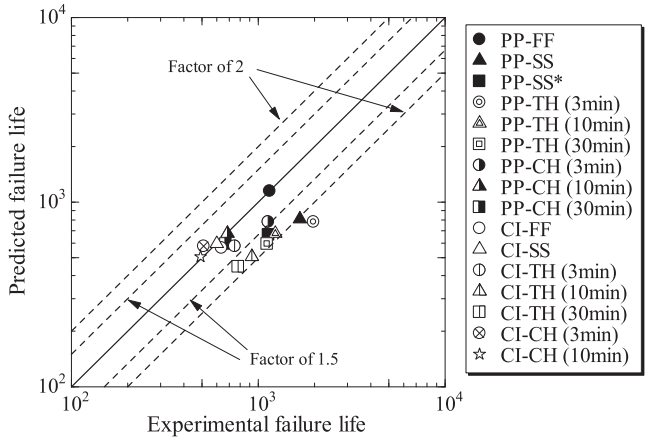

Fig. 8. Prediction by NMCFLE Method.

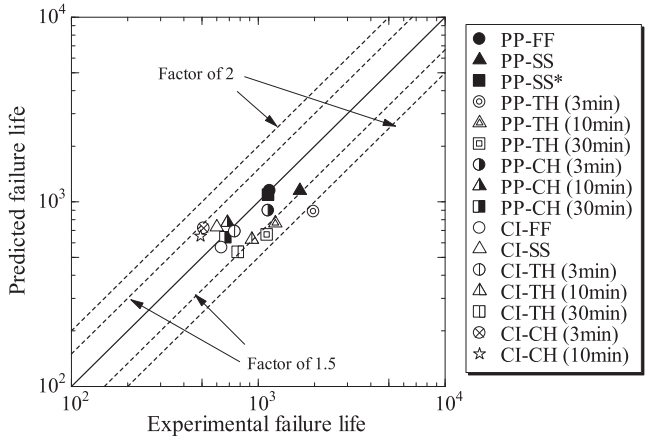

Fig. 9. Prediction by Mod NMCFLE Method.

with a small scatter within a factor of 1.5 for most of the tests regardless of the loading path, holding time, and strain rate.

Thus, the prediction accuracy of both the NMCFLE Method and the Mod NMCFLE Method is improved over that of the time fraction rule. In addition, the Mod NMCFLE Method showed the highest prediction accuracy.

5. Conclusions

In this paper, two types of multi-axial creep-fatigue life evaluation methods for non-proportional loading are proposed: the first one takes into account the effects of non-proportional loading and creep when calculating the strain range parameters using Manson's universal slope method. The second was to use the linear damage law to calculate fatigue damage using Manson's universal slope method and the non-proportional strain range, and to calculate creep damage using fracture ductility reduction rate. The failure life could be evaluated within a factor of 1.5 for most of the tests, and the improvement of prediction accuracy was confirmed.

Although the prediction accuracy of the NMCFLE method is lower than that of the Mod NMCFLE method, the Multiaxial Creep-Fatigue Life Evaluation Method is more convenient in terms of the ease of parameter calculation and the small amount of test data required. Therefore, it is appropriate to use the NMCFLE method for simple life prediction. Mod NMCFLE Method is suitable for more accurate life prediction with a smaller error.

These results indicate that the two evaluation methods proposed in this paper can satisfy a wide range of users' needs in terms of prediction accuracy and convenience of evaluation formulas.

Acknowledgements

The authors thank Ms. S. Noguchi and Mr. T. Sakurai in the University of Fukui for conducting the CI test, and Mr. K. Fukuike in Ritsumeikan University for assistance with the PP test. Dr. F. Ogawa acknowledges the support of The Iron and Steel Institute of Japan through ISIJ Research Promotion Grant.

REFERENCES

1) S. H. Doong, D. F. Socie and I. M. Robertson: *J. Eng. Mater. Technol.*, **112** (1990), 456. https://doi.org/10.1115/1.2903357
2) S. H. Doong and D. F. Socie: *J. Eng. Mater. Technol.*, **113** (1991), 23. https://doi.org/10.1115/1.2903379
3) C. H. Wang and M. W. Brown: *Fatigue Fract. Eng. Mater. Struct.*, **16** (1993), 1285. https://doi.org/10.1111/j.1460-2695.1993.tb00739.x
4) D. F. Socie and G. B. Marquis: Multiaxial Fatigue, Society of Automotive Engineers International, Warrendale, PA, (2000), 77.
5) F. Yousefi, M. Witt and H. Zenner: *Fatigue Fract. Eng. Mater. Struct.*, **24** (2001), 339. https://doi.org/10.1046/j.1460-2695.2001.00397.x
6) A. Nagesha, M. Valsan, R. Kannan, K. Bhanu Sankara Rao and S. L. Mannan: *Int. J. Fatigue*, **24** (2002), No. 12, 1285. https://doi.org/10.1016/S0142-1123(02)00035-X
7) T. Itoh, K. Murashima and T. Hirai: *J. Soc. Mater. Sci., Jpn.*, **56** (2007), No. 2, 157 (in Japanese). https://doi.org/10.2472/jsms.56.157
8) Y. Takahashi: *Int. J. Press. Vessel. Pip.*, **85** (2008), No. 6, 406. https://doi.org/10.1016/j.ijpvp.2007.11.008
9) K. Aoto: *Materia Jpn.*, **47** (2008), No. 9, 459 (in Japanese). https://doi.org/10.2320/materia.47.459
10) T. Kim, S. Zhang and M. Sakane: *Trans. Jpn. Soc. Mech. Eng. Ser. A*, **76** (2010), No. 768, 51 (in Japanese). https://doi.org/10.1299/kikaia.76.1059
11) T. Itoh and T. Yang: *Int. J. Fatigue*, **33** (2011), 1025. https://doi.org/10.1016/j.ijfatigue.2010.12.001
12) L. F. Coffin: Proc. 2nd Int. Conf. on Fracture, Chapman Hall, Brighton, London, (1969), 643.
13) S. S. Manson: *Exp. Mech.*, **5** (1965), No. 7, 193.
14) Y. Kadoya, T. Goto, K. Kawamoto and K. Sugai: *J. Soc. Mater. Sci., Jpn.*, **39** (1990), 516 (in Japanese). https://doi.org/10.2472/jsms.39.516
15) K. Tokimasa, K. Tanaka and I. Nitta: *J. Soc. Mater. Sci., Jpn.*, **35** (1986), No. 396, 1030 (in Japanese). https://doi.org/10.2472/jsms.35.1030
16) Y. Takahashi and M. Yaguchi: *J. Soc. Mater. Sci., Jpn.*, **54** (2005), No. 2, 168 (in Japanese). https://doi.org/10.2472/jsms.54.168
17) T. Itoh, K. Fukumoto, H. Hagi, A. Itoh and D. Saitoh: *J. Soc. Mater. Sci., Jpn.*, **62** (2013), No. 2, 110 (in Japanese). https://doi.org/10.2472/jsms.62.110
18) T. Itoh, M. Sakane and T. Morishita: *Frattura Integr. Strutt.*, **9** (2015), 289. https://doi.org/10.3221/IGF-ESIS.33.33
19) T. Itoh, M. Sakane, M. Ohnami and D. F. Socie: *J. Eng. Mater. Technol.*, **117** (1995), No. 3, 285. https://doi.org/10.1115/1.2804541
20) J. Zhou and T. Itoh: Proc. 50th Conf. Hokuriku-Shinetsu Branch, The Japan Society of Mechanical Engineers, Tokyo, (2013), 010401. https://doi.org/10.1299/jsmehs.2013.50.010401
21) X. Chen, Q. Gao and X.-F. Sun: *Fatigue Fract. Eng. Mater. Struct.*, **19** (1996), No. 7, 839. https://doi.org/10.1111/j.1460-2695.1996.tb01020.x
22) T. Itoh, T. Nakata, M. Sakane and M. Ohnami: *Eur. Struct. Integr. Soc.*, **25** (1999), 41. https://doi.org/10.1016/S1566-1369(99)80006-5
23) R. Plank and G. Kuhn: *Eng. Fract. Mech.*, **62** (1999), 203. https://doi.org/10.1016/S0013-7944(98)00097-6
24) T. Itoh, K. Murashima and T. Hirai: *J. Soc. Mater. Sci., Jpn.*, **56** (2007), No. 2, 157 (in Japanese). https://doi.org/10.2472/jsms.56.157
25) D. Saito, T. Itoh and K. Fukumoto: M & M Mechanics of Materials Conf., The Japan Society of Mechanical Engineers, Tokyo, (2011), OS0709 (in Japanese). https://doi.org/10.1299/jsmemm.2011._OS0709-1_
26) Y. Yin, T. Itoh and T. Kiya: M & M Mechanics of Materials Conf., The Japan Society of Mechanical Engineers, Tokyo, (2011), OS0703. https://doi.org/10.1299/jsmemm.2011._OS0703-1_
27) T. Ogata: *J. Soc. Mater. Sci., Jpn.*, **46** (1997), No. 1, 25 (in Japanese). https://doi.org/10.2472/jsms.46.25
28) Y. Kasamuta, F. Ogawa, T. Itoh and H. Tanigawa: MATEC Web Conf., Vol. 300, (2019), 07002. https://doi.org/10.1051/matecconf/201930007002